

## LASER MICROPROBE MASS ANALYSIS OF AMAZON BASIN AEROSOLS

L. WOUTERS, S. HAGEDOREN, I. DIERCK, P. ARTAXO\* and R. VAN GRIEKEN

University of Antwerp (UIA), Universiteitsplein 1, B-2610 Antwerp-Wilrijk, Belgium

(First received 15 June 1992 and in final form 6 November 1992)

**Abstract**—Individual aerosol particles sampled over the Amazon Basin, Brazil, were analysed using laser microprobe mass analysis (LAMMA). Spectra are complex due to the high organic content of the samples. Phosphate was found to be concentrated largely in one particle type, which was only detected in the dry season samples. This points to a biomass burning origin or at least to a season-related vegetative aerosol production mechanism. The most abundant particle type, most likely originating from a vegetation source, can be described as a mixture of different salts and organic fragments.

*Key word index:* Amazon, forest, aerosol, single particle analysis, LAMMA.

### INTRODUCTION

The samples analysed in this work were collected within the scope of the Amazon Boundary Layer Experiments (ABLE 2A and B) conducted in the Amazon Basin, Brazil (Harris *et al.*, 1988). The aim of these projects was to assess the role of biosphere-atmosphere interactions on the chemistry of the troposphere over tropical forests. They are part of a long-term study of the chemistry of the atmospheric boundary layer supported within the Global Tropospheric Experiment (GTE) of the NASA Tropospheric Chemistry Program.

It has been long known that vegetation can act as an aerosol source during burning activities (Andreae *et al.*, 1988a) and also by natural release, such as mechanical abrasion of plants leaves (Bigg and Twudy, 1978). Beaufort (1975) and Beaufort *et al.* (1977) showed that plants are capable of generating particulate Zn, Pb and Cu. Emitted plant wax particles contain trace amounts of K, P, Ca, Mg, Na and Cl (Wils *et al.*, 1981; Simoneit, 1984). According to Nemeruyk (1970), plant transpiration causes migration of  $\text{Ca}^{2+}$ ,  $\text{SO}_4^{2-}$ ,  $\text{Cl}^-$ ,  $\text{K}^+$ ,  $\text{Mg}^{2+}$  and  $\text{Na}^+$ . Of course, the nature and frequency of the emissions will depend largely on the plant itself and on meteorological factors, but generally, a forest ecosystem definitely influences the atmosphere.

The large-scale approach of the ABLE projects provided results that are suited for extrapolation and global budget calculations. Co-operation between different laboratories led to the determination of many parameters:  $\text{CO}_2$ ,  $\text{NO}$ ,  $\text{O}_3$ , NMHC (non-methane hydrocarbons), organic sulfur compounds (DMS, MSA), inorganic species, etc. (Harris *et al.*, 1988). Talbot *et al.* (1988), who participated in the

project, concluded that “the moist forest ecosystem is a source of aerosols, composed of material directly released by vegetation, together with species originating from biogenic emissions of various reduced atmospheric gases”. The aerosol over Amazonia was found to be composed primarily of organic compounds. It exhibits a neutral ionic character, primarily due to incorporation of  $\text{NH}_4^+$ , presumably derived from  $\text{NH}_3$  released by the forest ecosystem.

To complement the bulk measurements, single particles were analysed in the present work, in an attempt to obtain even more detailed information about the origin of the particles. Two different techniques were used: electron-probe X-ray microanalysis (EPXMA), the results of which have been presented elsewhere (Artaxo *et al.*, 1988), and laser microprobe mass analysis (LAMMA). These two techniques can be considered largely complementary: using EPXMA, particles can be analysed automatically for their major element composition, but elements with  $Z < 11$  cannot be detected. LAMMA, on the other hand, can detect all elements (and detection limits are generally at least a factor of 10 better) but it is not automated and suffers more from spectral interferences.

### EXPERIMENTAL

#### Sampling

All samples analysed are described in Table 1. The samples L4AM and L5AM are characteristic for the dry season. They were sampled on the top of a 45-m high meteorological tower (that extends through the canopy) located in the Ducke nature reserve, 20 km northeast of Manaus, Brazil. The aerosols were collected using a 10-stage Batelle-type impactor with aerodynamic cut-off diameters of 16, 8, 4, 2, 1, 0.5, 0.25, 0.12 and 0.06  $\mu\text{m}$  and a back-up filter, equipped with Formvar-coated electron microscope grids. It was operated at a flow rate of  $1 \text{ l min}^{-1}$ . Meteorological conditions were the same for both dry season samples; wind direction during

\* On leave from Institute of Physics, University of São Paulo, São Paulo, Brazil.

Table 1. Sample description

Sample	Sampling date	Altitude (range) (m)	Coordinates (range)
L4AM	6.8.85	45	2°57'S 59°57'W
L5AM	8.8.85	45	2°57'S 59°57'W
ICA13	29.4.87	4270–3960	2°32'–3°18'S 59°30'–58°54'W
ICA14	29.4.87	1830–1520	2°34'–2°38'S 58°48'–59°50'W
ICA15	29.4.87	210–300	2°41'–2°42'S 58°42'–59°44'W
ICA16	29.4.87	1210–1210	2°23'–2°45'S 59°24'–59°24'W

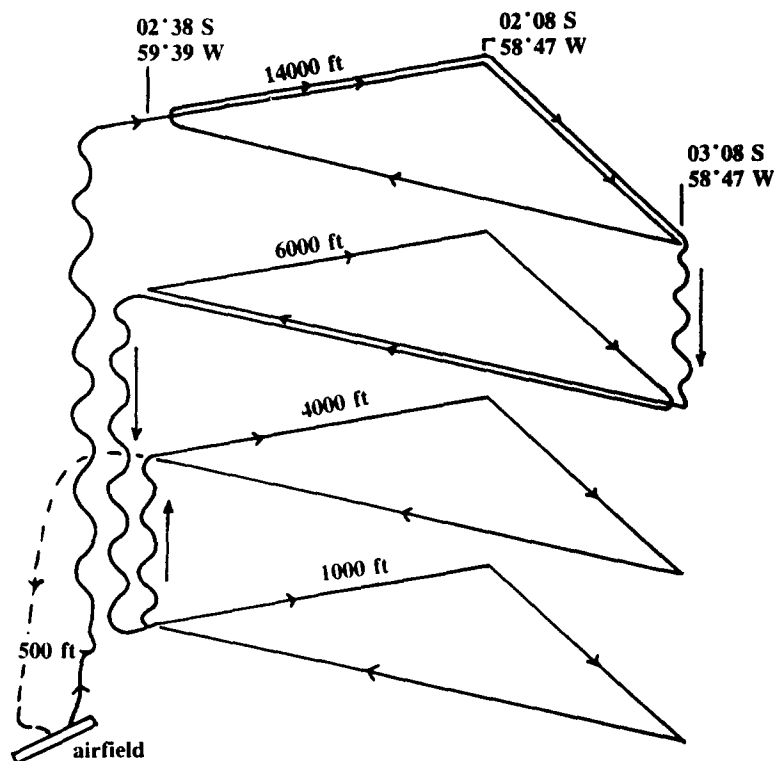


Fig. 1. Proposed flight scheme for ABLE 2B (1 ft = 0.3048 m).

sampling was north to northeast, so the sampled air passed through forested areas for at least some 200 km and it can thus be considered forestal.

The wet period samples (ICA13–16) were collected during a flight of a NASA Lockheed Electra aircraft over the Amazon Basin. The flight scheme is represented in Fig. 1. Sampling was performed with the same impactor as in the dry season aerosol.

Before analysis, the samples were stored in sealed petri dishes.

#### LAMMA instrumentation

In the LAMMA-500 instrument (Leybold-Heraeus, Cologne, F.R.G.), individual aerosol particles are vaporized by a single high-power laser pulse ( $\tau = 15$  ns) of a Q-switched frequency quadrupled Nd:YAG laser ( $\lambda = 265$  nm, power density =  $10^7 - 10^{11}$  W cm $^{-2}$ ). The resulting microplasma contains atomic and molecular ions, as well as electrically neutral fragments. Depending on the spectrum polarity chosen, positive or negative ions are accelerated and collimated into the drift tube of a time-of-flight mass spectro-

meter where they are separated according to their  $m/z$  ratios. The signal is then fed into a 32-Kbyte memory transient recorder (Lecroy TR8818) and digitized. Spectra are stored using a personal computer for off-line data handling. Groups of spectra can be automatically calibrated, integrated and compared to a library of standard spectra, which can be complemented by the user. All software applied is home-made. The instrument and the software package are discussed extensively in the literature (Verbueken *et al.*, 1988; Van Espen *et al.*, 1986).

#### RESULTS AND DISCUSSION

The Amazon Basin aerosol spectra are very complicated. This is due to the overwhelming presence of organics (according to Talbot *et al.*, 1988, more than 80% of the aerosol mass). Single particle analysis performed on similar samples with EPXMA (Artaxo *et al.*, 1988) revealed the presence of essentially four

particle types: K-(S)-(P)-(Cl)-rich particles with a high Bremsstrahlung background, indicating that they are rich in organic material; silicates; K-Ca-S-Na-(Cl)-rich particles; and a group exhibiting only sulfur-peaks in their X-ray spectra, possibly ammonium sulfate.

Although sampling was performed with a 10-stage impactor, not every stage was analysed. The reasons are manifold: some particles were too big to be properly analysed by LAMMA, some grids had too low load and some grids were destroyed during sampling or shipping. For every analysed impactor stage, roughly 100 spectra were recorded; *ca* 50 in both the positive mode and the negative mode. In this way, some 2200 spectra were obtained. To handle them in an efficient way, a home-made computer program based on the library search concept (Martinsen, 1981) was used. Compounds and patterns to be included in the search routine were selected upon manual inspection of several random samples and data from the literature. Because of the complexity of part of the spectra, extreme care was taken to avoid misclassification.

Part of these particles appear as internal mixtures. Therefore, overlap is permitted in the classification proposed in the following paragraphs (e.g. a particle containing both ammonium and phosphate peaks will be classified as ammonium-rich and also as phosphate-rich).

#### Dry season samples

Especially among the bigger particles, aluminosilicates are rather abundant. Figure 2a represents their abundances as a function of particle size (i.e. impactor stage), averaged over the two impactors (L4AM and L5AM). The stages 7-3 correspond to aerodynamic cut-off diameters of, respectively, 0.25, 0.5, 1, 2 and 4  $\mu\text{m}$ . Their size distribution suggest a soil dust origin. Particles whose spectra show Si and, Si-O cluster but no Al, appear very often in the smallest size range (Fig. 2b). These silicon-rich particles were also detected with EPXMA in similar samples (Artaxo *et al.*, 1988). Up to now, their origin is not clear.

Figure 3 shows a representative positive mode spectrum and the size distribution of the frequently appearing salt particles. "Salt", in this context, refers to particles whose positive mode spectra look like mixtures of several salts: sulfates, carbonates, chlorides and sometimes nitrates and phosphates. At first sight, they are very similar to the spectra of sea salt transformed in the atmosphere (Wouters *et al.*, 1990). The only differences lie in their significantly higher calcium content, the appearance of  $\text{Ca}_x\text{O}_y$  clusters and occasionally of  $\text{PO}^+$ . Negative mode spectra often show quite intense small organic fragments. These particles are most likely not sea-salt-derived. According to Talbot *et al.* (1988), the main influence of sea salt on the aerosol composition over the forest extends

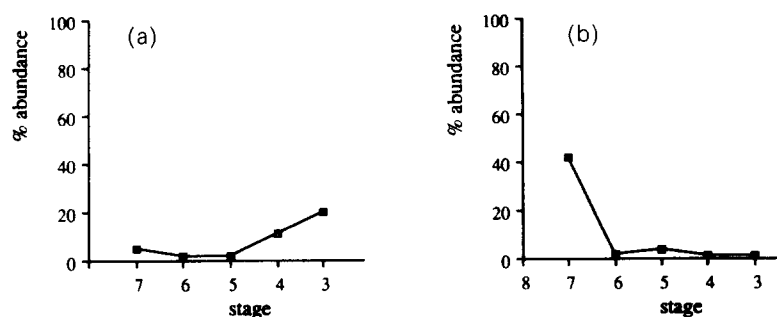


Fig. 2. Relative abundances of (a) aluminosilicate particles and (b) silicon-rich particles as a function of particle size.

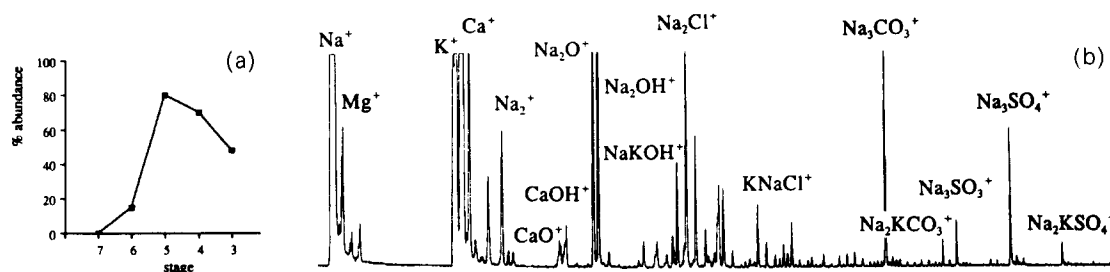


Fig. 3. Salt particles: representative positive mode spectrum and relative abundance as a function of particle size.

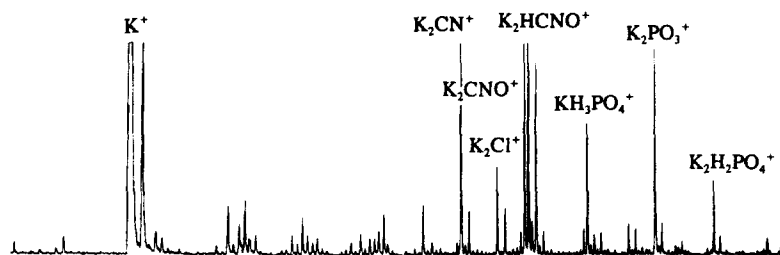


Fig. 4. Representative positive mode spectrum of a potassium-rich particle.

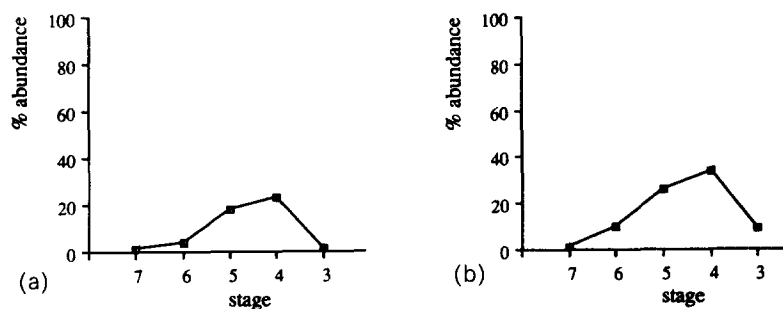


Fig. 5. Relative abundances of (a) potassium-rich particles and (b) particles whose spectra exhibit (H)PO<sub>x</sub> clusters as a function of particle size.

about 400 km inland and this aerosol was sampled 1000 km away from the ocean. The most plausible explanation for this particle type is emission products from leaf surfaces. These spectra do correspond with the findings of Nemeruyk (1970), who stated that migration of Ca<sup>2+</sup>, Na<sup>+</sup>, Mg<sup>2+</sup>, K<sup>+</sup>, HCO<sub>3</sub><sup>-</sup>, SO<sub>4</sub><sup>2-</sup> and Cl<sup>-</sup> takes place during crop plant transpiration.

A special kind of spectral pattern, hitherto only encountered in this tropical forest aerosol, is attributed to potassium-rich particles. Positive mode spectra are characterized by very intense potassium-peaks and K(-H)-PO<sub>x</sub>, K-Cl and K-CN(O) clusters. Negative mode spectra show (H)PO<sub>x</sub><sup>-</sup>, CN(O)<sup>-</sup>, small organic clusters and often SO<sub>x</sub><sup>-</sup> clusters and Cl<sup>-</sup> peaks. A representative positive ion spectrum and the size distribution curves for both the K(-H)-PO<sub>x</sub><sup>+</sup> and (H)PO<sub>x</sub><sup>-</sup> clusters are presented in Figs 4, 5a and 5b, respectively. The resemblance between these two curves points to the fact that the major part of the phosphate is associated with this particle type. Variations can be attributed to a minor association with the salt particles (previous paragraph), to the (from a statistical point of view) limited number of analyses (two times *ca* 50) and to differences in the sensitivities of K(-H)-PO and PO<sub>x</sub><sup>-</sup> clusters. Although the K-P-O part of the spectra highly resembles that of a KH<sub>2</sub>PO<sub>4</sub> standard, an organic (e.g. phospholipid) source also seems possible in this case because of the above-mentioned appearance of small organic fragments. Lawson and Winchester (1979) found K, P and S in a tropical rain forest to be closely associated and to appear primarily in the coarse (> 1 μm) mode. They

attributed these elements to a vegetation source. As 70% of these particles do not exhibit other peaks than the ones described above, this would imply the existence of two different particle types (i.e. salt and potassium-rich) originating from a similar source.

The metal-rich group contains predominantly Cr/Fe/Pb- and Ti-rich particles. Beaufort *et al.* (1977) showed that plants are capable of emitting heavy elements such as zinc and lead. But then, roughly 60% of these particles show no peaks other than the metal (oxide)-related ones and there does not seem to be a reason to assume that heavy metals should be emitted separately from the biologically important elements such as Mg, Ca, K and Na. This, and the fact that their relative abundances are rather low (Fig. 6) points to an anthropogenic origin.

The conjugated base of methane sulfonic acid (MSA) was frequently detected in these aerosols, especially among the smallest particles. Until recently, this species was believed to originate exclusively from the photochemical oxidation of organic sulfur products (DSM, MeSH) that are emitted by oceanic and continental ecosystems (Andreae *et al.*, 1986; Lovelock *et al.*, 1972). Recent laboratory studies, however, suggest that MSA is also released during biomass burning. MSA can be detected in both positive and negative mode spectra as Na<sub>2</sub>(CH<sub>3</sub>SO<sub>3</sub>)<sup>+</sup>, NaK(CH<sub>3</sub>SO<sub>3</sub>)<sup>+</sup> and CH<sub>3</sub>SO<sub>3</sub><sup>-</sup>. Size distributions based on positive and negative mode spectra follow the same trend: MSA is clearly concentrated on the smallest particles (Figs 7a and 7b). Heterogeneous nucleation reactions

and/or adsorption effects are responsible for the presence of MSA in the particulate fraction. MSA occurs together with  $(\text{H})\text{SO}_4^-$  ions in the negative mode, and with  $\text{NH}_4^+$  or sometimes "salt spectra" (see previous paragraph) ions in the positive mode spectra. Therefore, possible counterions are  $\text{NH}_4^+$ ,  $\text{Na}^+$ ,  $\text{K}^+$ ,  $\text{Mg}^{2+}$  or  $\text{Ca}^{2+}$ . The insensitivity of LAMMA towards  $\text{NH}_4^+$  might obscure its importance as a counterion, but Andreae and Andreae (1988) believe that ammonium salts of organic acids are too volatile to form stable aerosols.

The ammonium ion is often detected among the smallest particles (Fig. 8). The reduced relative abundance on stage 7 compared to stage 6 is due to the unexplained presence of Si-rich particles on the former. According to Andreae *et al.* (1988b) it is the principal ionic constituent present at a concentration of more than twice that of other major ionic species. The substantial aerosol  $\text{NH}_4^+$  concentration arises from chemical transformation of atmospheric  $\text{NH}_3$ . Sources of  $\text{NH}_3$  are emissions from the forest and wetlands. From the negative mode spectra, plausible candidates for counterions are  $\text{SO}_4^{2-}$  or maybe organics, but then, as already mentioned in a previous paragraph, ammonium-salt of organic acids are too volatile to form stable aerosols. Andreae *et al.*

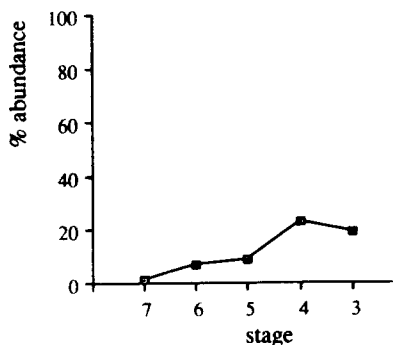
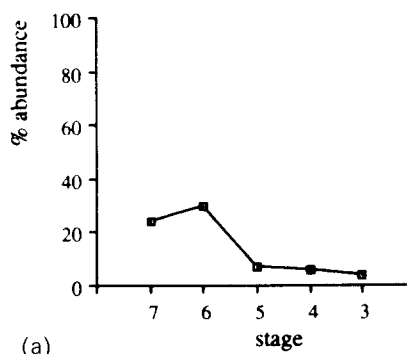


Fig. 6. Relative abundance of metal-rich particles as a function of particle size.



(1988b) believe that free organic acids are retained in the aerosol by adsorption. On the other hand,  $\text{NH}_4^+$  is also a common small fragment of amino acids, as appears from analysis of pure compounds.

Nitrate does not appear too often in these spectra. This might be a consequence of prolonged storage: nitrates are not stable and the particles were analysed some 4 years after sampling took place. The size distribution, based on the appearance of  $\text{NO}_3^-$  ( $x=2$  and 3) peaks in the negative mode spectra, is shown in Fig. 9. Nitrate was found to be associated with salt particles, but also with aluminosilicates. It is mostly detected in the coarse mode. This corresponds with the findings of Talbot *et al.* (1988) who found 75% of the total aerosol  $\text{NO}_3^-$  to be contained in the coarse fraction ( $> 1 \mu\text{m}$ ). Theoretical considerations also led to the same result (Basset and Seinfeld, 1984). Just as ammonium, nitrate is believed to originate from emissions of N-containing gases from the forest ecosystem. Incorporation in the aerosol occurs by the reaction of atmospheric nitric acid with particulates. As is sometimes detected in salt spectra, direct emission from the vegetation is another possible source for part of the nitrate.

The huge organic content of this aerosol is especially apparent in the negative mode spectra, which show a frequent and very intensive appearance of, most of the time, small organic fragments such as  $\text{CN}^-$ ,  $\text{CNO}^-$ ,  $\text{HCNO}^-$ ,  $\text{HCOO}^-$ ,  $\text{CH}_3\text{COO}^-$ ,  $\text{C}_x\text{H}_y^-$  ( $x < 3, y < 7$ ), etc. These fragments have, however, little or no decisive value for compound determination. They appear in all particle types detected but most frequently in MSA-, potassium- and salt-rich particles. Their intensities are highest in the smallest size ranges. As an example, Fig. 10 shows the size distribution of negative mode spectra in which both the  $\text{HCOO}^-$  and  $\text{CH}_3\text{COO}^-$  clusters are dominant, or at least comparable to other dominant peaks in the spectra.

#### Wet season samples

Wet season aerosol spectra can be divided into the same groups as the dry season ones, with one exception: the potassium-rich particles (defined in the

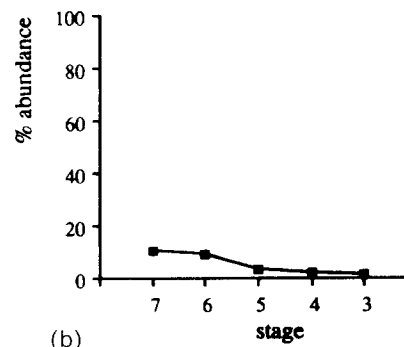


Fig. 7. Relative abundances of particles whose spectra exhibit MSA-related peaks (a) in the negative mode and (b) in the positive mode as a function of particle size.

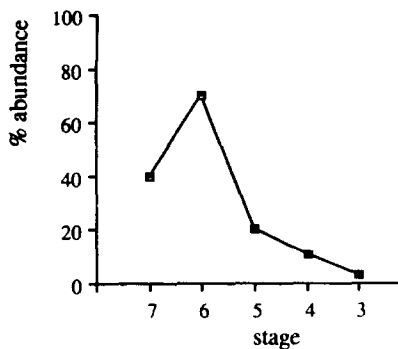


Fig. 8. Relative abundance of NH<sub>4</sub><sup>+</sup>-containing particles as a function of particle size.

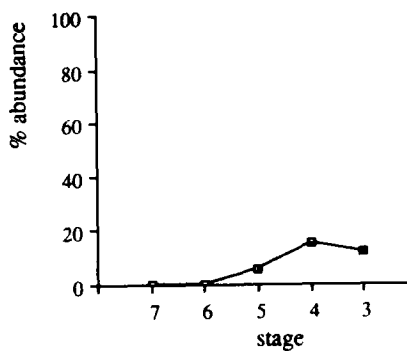


Fig. 9. Relative abundance of NO<sub>3</sub><sup>-</sup>-containing particles as a function of particle size.

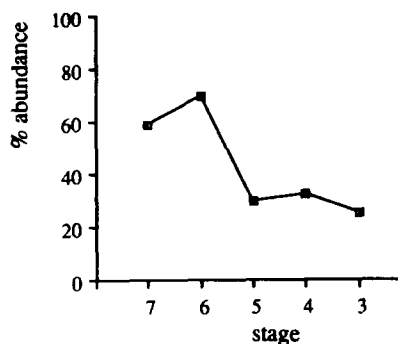


Fig. 10. Relative abundance of particles whose spectra exhibit acetate fragments as a function of particle size.

former section) were not detected any more in this case. As biomass burning activities do not take place during this time of year, this might imply a vegetation burning source. Andreae *et al.* (1988a) do report elevated potassium-concentrations (up to a factor of three) in biomass burning haze, but they do not mention data on phosphorus.

Except for the highest air masses, aluminosilicates are clearly relatively more present in the coarser

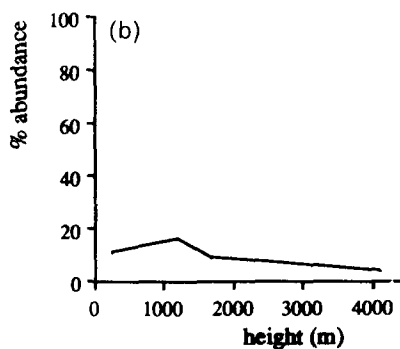
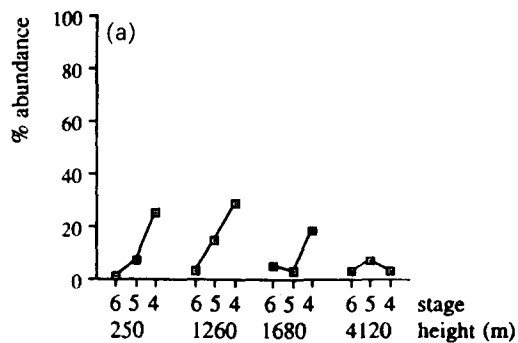


Fig. 11. Relative abundance of aluminosilicates (a) as a function of particle size and (b) as a function of height.

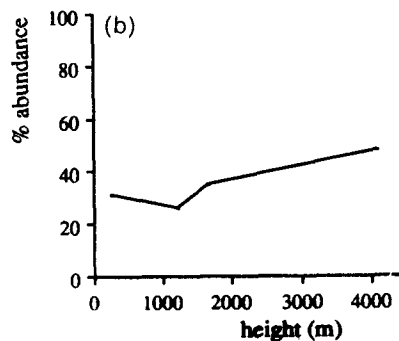
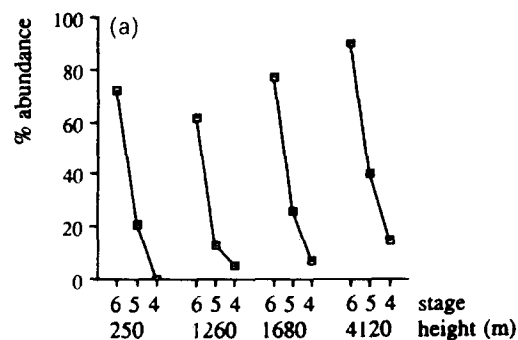


Fig. 12. Relative abundance of NH<sub>4</sub><sup>+</sup>-containing particles (a) as a function of particle size and (b) as a function of height.

particles (Fig. 11a). Their relative abundances show an overall decrease as a function of sampling height (Fig. 11b). Particles whose spectra show Si(-O) clusters but no Al are also sporadically detected in this case, but they follow no specific trends as a function of particle size.

Ammonium-containing particles prevail in the smallest size range (Fig. 12a). Their relative abundances increase slightly with increasing height (Fig. 12b). Particles whose spectra are dominated by small organic clusters follow the same trend (Figs 13a and 13b).

MSA-related peaks are sporadically detected, but their abundances are too low to draw final conclusions about them.

Just as for the dry season samples, salt particles generally have their lowest abundances in the sub-micrometer range, except for the impactor sampled at an altitude of 1680 m (Fig. 14a). Their relative abundances do not change significantly with sampling height (Fig. 14b).

Heavy metal-rich particles seem to follow a similar trend, although their overall abundance is much lower than that of the salt particles (Figs 15a and 15b).

#### Dry season vs wet season samples

Comparing these two aerosols, one should keep in mind that the dry season samples were approximately 2 years older than the wet season samples at the time of analysis.

The major difference between these samples was already mentioned in the former section: Potassium-rich particles, described for the dry season samples, were never detected in the wet season aerosol. This points to a biomass burning origin or at least to season-related differences in vegetative aerosol production. Furthermore, the MSA-related compounds have a much lower incidence in the wet season samples. The so far unexplained silicon-enrichment in the smallest dry season particles did not occur for the wet season. For the other particle types and/or compounds, there are neither marked differences in relative abundance, nor in size distribution, between dry season and the wet season particles, when sampled at the lowest altitude. Possibly, absolute abundances would bring in more conclusive results concerning wet deposition efficiency, but it was impossible to obtain those with the parameters provided by the sampling campaign.

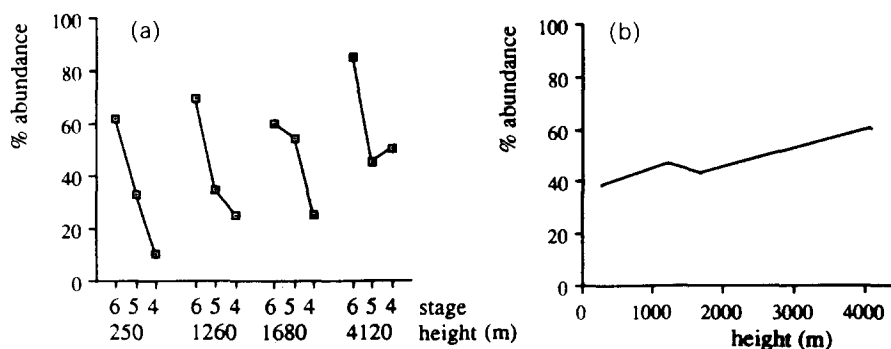


Fig. 13. Relative abundance of acetate-containing particles (a) as a function of particle size and (b) as a function of height.

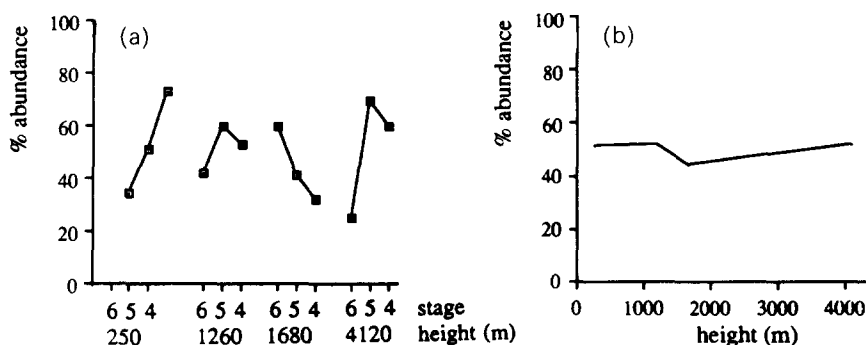


Fig. 14. Relative abundance of salt particles (a) as a function of particle size and (b) as a function of height.

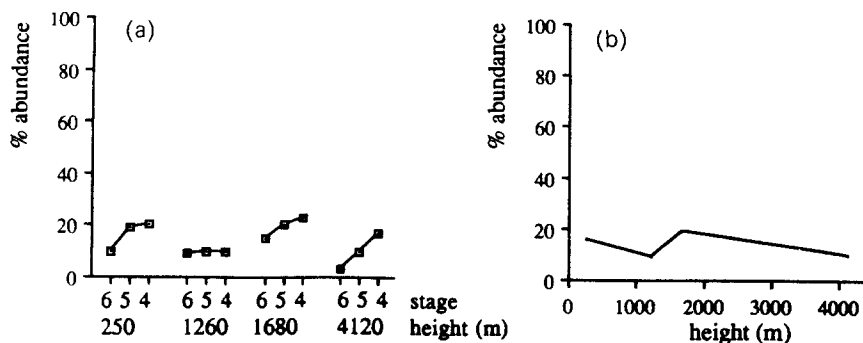


Fig. 15. Relative abundance of heavy metal-containing particles (a) as a function of particle size and (b) as a function of height.

### CONCLUSION

Single particle analysis definitely adds to the information obtained by bulk analysis, especially in the source apportionment field.

In this particular case, phosphate was found to be concentrated largely in one particle type, which was not detected in the wet season samples. This points to a biomass burning origin or at least to season-related vegetative aerosol production mechanisms. Heavy metal-rich particles were considered anthropogenic on the base of the absence of significant mass peaks, other than the metal-oxide-related ones in their spectra. The most abundant particle type, most likely originating from a vegetation source, can be described as a mixture of different salts and organic fragments.

In order to obtain even more conclusive results concerning particle sources, the use of small-scale model ecosystem would be very helpful. A simulation of dry and wet season conditions and biomass burning could then provide more suitable particle standards for the library search routine.

### REFERENCES

- Andreae M. O. and Andreae T. W. (1988) The cycle of biogenic sulfur compounds over the Amazon Basin: 1. Dry season. *J. geophys. Res.* **93**, 1487–1497.
- Andreae M. O., Charlson R. J., Bruynseels F., Storms H., Van Grieken R. and Maenhaut W. (1986) Internal mixture of sea salt, silicates and excess sulfate in marine aerosols. *Science* **232**, 1620.
- Andreae M. O., Browell E. V., Garstang M., Gregory G. L., Harris R. C., Hill G. F., Jacob D. J., Pereira M. C., Sachse G. W., Setzer A. W., Silva Dias P. L., Talbot R. W., Torres A. L. and Wofsy S. C. (1988a) Biomass-burning emissions and associated haze layers over Amazonia. *J. geophys. Res.* **93**, 1509–1527.
- Andreae M. O., Talbot R. W., Andreae T. W. and Harris R. C. (1988b) Formic and acetic acid over the central Amazon region, Brazil: 1. Dry season. *J. geophys. Res.* **93**, 1616–1624.
- Artaxo P., Storms H., Bruynseels F., Van Grieken R. and Maenhaut W. (1988) Composition and sources of aerosols from the Amazon Basin. *J. geophys. Res.* **93**, 1605–1615.
- Bassett M. E. and Seinfeld J. H. (1984) Atmospheric equilibrium model of sulfate and nitrate aerosols — II. Particle size analysis. *Atmospheric Environment* **18**, 1163–1170.
- Beaufort W. (1975) Heavy metal release from plants into the atmosphere. *Nature* **256**, 35.
- Beaufort W., Barber J. and Barringer A. (1977) Release of particles containing metals from vegetation into the atmosphere. *Science* **195**, 571–573.
- Bigg E. K. and Turvey D. E. (1978) Sources of atmospheric particles over Australia. *Atmospheric Environment* **12**, 1643–1655.
- Harris R. C., Wofsy S. C., Grastang M., Browell E. V., Molion C. B., McNeal R. J., Hoell J. M., Bendura R. J., Beck S. M., Navarro R. L., Riley J. T., and Snell R. L. (1988) The Amazon Boundary Layer Experiment (ABLE 2A): dry season 1985. *J. geophys. Res.* **93**, 1351–1360.
- Lawson D. R. and Winchester J. W. (1979) Sulfur, potassium and phosphorus associations in aerosols from South American tropical rain forest. *J. geophys. Res.* **84**, 3723–3727.
- Lovelock J., Maggs R. and Rasmussen R. (1972) Atmospheric dimethyl sulphide and the natural sulphur cycle. *Nature* **237**, 452.
- Martinsen D. P. (1981) Survey of computer aided methods for mass spectral interpretation. *Appl. Spectr.* **35**, 255–266.
- Nemeruyk G. (1970) Migration of salts in the atmosphere during transpiration. *Soviet Plant Physiology* **17**, 560–566.
- Simoneit B. R. T. (1984) Application of molecular marker analysis to reconcile sources of carbonaceous particulates in tropospheric aerosols. *Sci. Total Envir.* **36**, 61–72.
- Talbot R. W., Andreae M. O., Andreae T. W. and Harris R. C. (1988) Regional aerosol chemistry of the Amazon Basin during the dry season. *J. geophys. Res.* **93**, 1499–1508.
- Van Espen P., Van Vaeck L. and Adams F. (1986) In *Proc 3rd Int. LAMMS Workshop* (edited by Van Vaeck L. and Adams F.), pp. 195–198. University of Antwerp.
- Verbueken A., Bruynseels F. and Van Grieken R. (1988) In *Inorganic Mass Spectrometry* (edited by Adams F., Gijbels R. and Van Grieken R.), pp. 173–257. Wiley, New York.
- Wils R., Hulst A. and Hartog J. (1981) The occurrence of plant wax constituents in airborne particulate matter in an urbanized area. *Chemosphere* **11**, 1087–1096.
- Wouters L., Artaxo P. and Van Grieken R. (1990) Laser microprobe mass analysis of individual antarctic aerosol particles. *Int. J. envir. analyt. Chem.* **38**, 427–438.